The Large-Area Picosecond Photon Detector (LAPPD^{TM}), an Ideal Tool for Quantum Optics

B.W. Adams[*,1,2]**, E. Angelico**[2]**, M. Aviles**[1]**, J.L. Bond**[1]**, C.A. Craven**[1]**, T. Cremer**[1]**, M.R. Foley**[1]**, H.J. Frisch**[2]**, A.V. Lyashenko**[1]**, M.J. Minot**[1]**, M.A. Popecki**[1]**, M. Stokaj**[1]**, W.A. Worstell**[1]

[1]*Incom, Inc., Charlton, MA 01507, U.S.*
[2]*Enrico Fermi Institute, the University of Chicago*
E-mail: badams@incomusa.com

The large-area picosecond photodetector (LAPPD^{TM}) is an ultrafast imaging detector with single-photon sensitivity. The time resolution approaches the coherence time of light filtered with dielectric-layer interference filters, and so, the detector can resolve photon occupations in each longitudinal mode of light. Furthermore, if used with diffraction-limited optics matched to the spatial resolution, the detector can also resolve about 400 by 400 transverse modes. LAPPD^{TM} is thus an enabling technology for quantum optics where photon occupation numbers in each electromagnetic-field mode in 6-dimensional phase space are relevant, for example photon-correlation experiments (Hanbury Brown - Twiss, or ghost imaging).

---

[*]Speaker.

1. Introduction

Quantum optics is largely the study of quantum correlations in the electromagnetic field (EMF), which give information on the matter with which the EMF interacts on the way from generation to detection. These quantum correlations may come in the form of straight-out photon correlation measurements, such as in the Hanbury Brown - Twiss experiment [1], or in photon detection correlated with a trigger signal. The latter usually comes in the form of a laser or radio-frequency (RF) pulse, which can also be seen as photon detection (typically, multi-photon detection). In the context of linear optics, the EMF can be described in terms of of electromagnetic-field modes (EMM) given by the boundary conditions, photon occupations of the EMM, and quantum correlations between them. The boundary conditions defining the modes are given by conductors and dielectrics forming walls, optical elements, etc.

It is thus important to be able to measure the photon occupations on a mode-by-mode basis. In the paraxial approximation, i.e., when one can describe an experiment in terms of a beam axis, and two-dimensional positions and angles relative to it, one can discuss this in terms of transverse and longitudinal modes. When optics are used that produce diffraction-limited spots on a sensor that correspond to the pixel size, then the sensor will resolve transverse modes given by the pixel area and conjugate diffractive solid angle. Likewise, when the spectral bandwidth of the light is restricted to yield a coherence time corresponding to the time resolution of the detector, then longitudinal modes are resolved. It is not sufficient to resolve only transverse modes because light arriving at time differences beyond the spectrally given coherence time is, generally, incoherent. Likewise, it is not sufficient to only resolve longitudinal modes because light arriving simultaneously, but in different locations outside of the diffraction-limit is also, generally, incoherent.

For a full resolution of the photon occupations, one needs to consider both the transverse, and the longitudinal modes. The volume in optical phase space that can be measured consists then of that of uncertainty-product (or Fourier-transform) cells times the number of pixels times the number of time slices that the detector can process separately.

2. LAPPD^{TM}

The Large-Area Picosecond Photon Detector (LAPPD^{TM}) was developed [2] by a consortium of universities, national laboratories, and industry with the goal of satisfying needs of the particle-physics community. Among these are precision timing of collision events and neutrino physics where large areas on the wall of vessels producing Cerenkov and scintillation light need to be covered with spatially and temporally resolving light sensors. The detector technology that came out of this project turns out to be well suited for other application areas, such as medical imaging including time-of-flight positron-emission tomography (TOF-PET), photon-timing imaging such as imaging LIDAR, or quantum optics.

Among light sensors, LAPPD^{TM} is distinguished by sensing at the single-photon level on a large area (20 cm by 20 cm) with a good spatial resolution (sub-mm in two dimensions), at a high time resolution (currently 50 ps), and with very low dark-count rates of the order of thousands of events per second on the entire sensor area, i.e., less than one per second and mm^2.

LAPPD^{TM} devices consist of a photocathode and a stack of microchannel plates in a flat-panel vacuum package. Fig. 1 shows a schematic of the a first-generation LAPPD^{TM} device. In
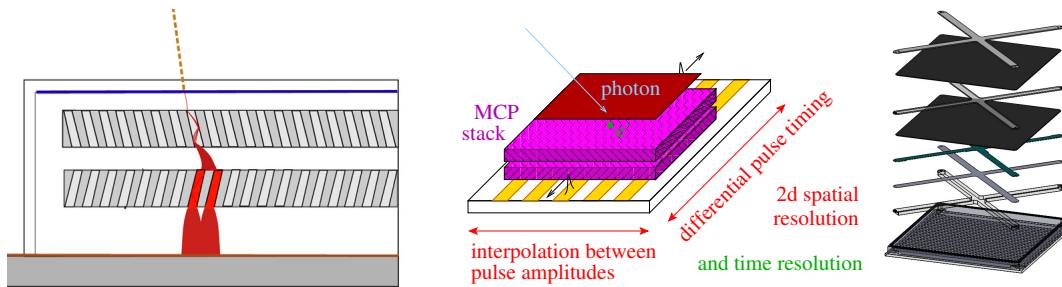

Figure 1: Left: Schematic side view of a Gen-I LAPPD: Photons on a photocathode eject photoelectrons, which are then amplified about a million-fold in a stack of microchannel plates. The amplified pulse hits a patterned readout anode. Center: In the case of generation I, the anode consists of an array of microwave striplines on which the amplified current pulses spread bilaterally to be sampled on the detector edges by fast (10 Gsamples/s) waveform digitizers. The figure on the right shows a schemtic of the stackup of microchannel plates inside the glass "tile" of the LAPPD^{TM}. Device dimensions are 20 cm by 20 cm laterally, and about 20 mm in thickness.

this device, photons release photoelectrons from a photocathode. These are accelerated to a stack of microchannel plates, where amplification by, typically, a factor of 10^6 produces measurable current pulses that hit a patterned readout anode. In the Gen-I design, the anode consists of an array of microwave striplines where the currents spread bilaterally, to be sampled by fast waveform digitizers. The timing of a photon then comes directly from the waveforms, the location along the striplines from the differential signal timing, and the location in the transverse direction from interpolation of the signal amplitudes between striplines. The striplines have, nominally, 50-Ohm impedance given by their width, and the nature and thickness of the dielectric underneath, which is part of the vacuum package. Timing and spatial resolution of this design were characterized [3, 4, 5] using devices with an aluminum photocathode, which could be easily removed in air to re-configure the MCP stackup, etc. Apart from the cathode, the devices were full-scale assemblies of all other components. Protoype production [6] of fully vacuum-sealed Gen-I devices with, typically, bi-alkali photocathodes for visible-light sensitivity is being pursued at the Incom R&D facility. To date, two fully functional prototype devices of the Gen-I design have been produced. Generation-II, currently under development, will likely employ capcitive signal coupling, so the readout-anode pattern is outside of the vacuum package.

3. The Hanbury Brown - Twiss Experiment

The famous Hanbury Brown - Twiss (HBT) experiment [1] demonstrates the importance of a high time resolution, and thus a potential application area of the LAPPD^{TM}, and also serves as a lead-in to other applications. HBT, i.e., intensity interferometry with light of thermal photon statistics sits at the interface of classical and quantum physics. For the sake of clarity, we will discuss a slight variation of the original experiment [1], which was to measure the angular diameter of a stellar disk (Sirius A), i.e., a source spanning a contiguous solid angle. Instead, assume that the task is to measure the angular separation of the components of a binary star, or, for that matter, of

two stars that are separated by light-years, and just happen to almost line up on the sky, as is shown in Fig. 2. To an individual telescope, the stars appear as a single point source, i.e., their angular
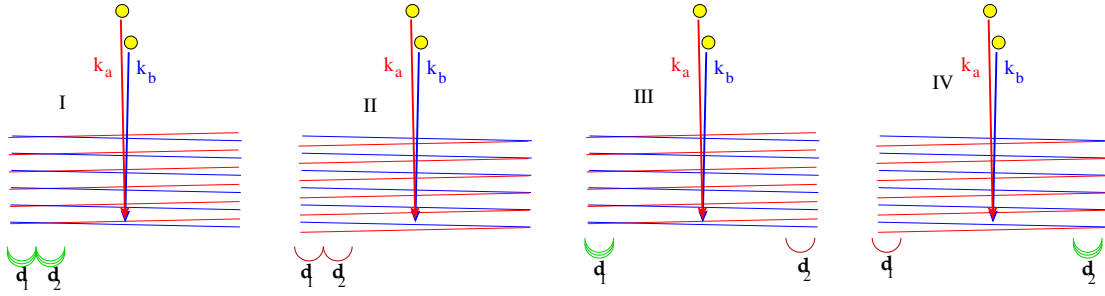

Figure 2: Schematic representation of HBT intensity interference. Shown are standing-wave patterns due to pairs of plane waves from distant stellar sources. These interference patterns persist for as long as the coherence time of the light, which is given by the spectral filtering. Detectors (half-circles) have a large probability of registering a photon (indicated by the "ringing") when they are in a momentary interference maximum of the pattern. Shown are four configurations with different detector positions and different states of interference. In graphs 1I and II, both detectors are close together,a nd in III and IV they are separated by a distance equal to half of the period of the interference pattern. Graphs I and III show a moment of constructive interference on the left, and II and IV a moment of constructive interference on the right. See also text.

separation on the sky is below the resolution limit. The resolution can be improved by increasing the telescope aperture, or by combining the light from two telescopes interferometrically. The latter approach is far from trivial because the optical paths of 10s to 100s of meters must be matched to sub-micron precision, all the while tracking against Earth's rotation. The interference of light coming by way of the two telescopes produces a pattern of interference stripes with a period that is reciprocal to the angular separation of the sources. Due to atmospheric density fluctuations, the pattern moves rapidly, and thus is hard to detect.

In an HBT experiment, the light intensities are measured right at the telescopes, and the resulting signals are correlated electronically. Even though the light amplitudes on the two stars are not correlated in any way, their fluctuations seen on Earth are greatly constrained because the light is present in only two electromagnetic-field modes (here, well approximated by plane waves): if the electromagnetic amplitude is known at some point in a plane wave, it is known everywhere in a plane perpendicular to the propagation direction. Furthermore, the amplitude is also determined along the propagation direction over a distance given by the coherence time resulting from the spectral bandwidth set by filters, etc. The two plane waves set up an interference pattern that fluctuates on time scales set by the spectral filtering. If the two detectors are close together (graphs I and II in Fig. 2), then detection events are correlated between them: whenever the interference is constructive at their location, there is a high probability of both detectors registering a photon, and if it is destructive, then neither will register a photon. However, if the two detectors are separated by a distance of half the period of the interference pattern (III and IV in Fig. 2), then, whenever the interference is constructive at the location of one, it is destructive at the other, and vice versa. Of course, interference at one detector location may be partially constructive (relative phase angle $\neq 0, \pi$), and then it is also partially constructive at the other, so both detectors may still see corre-

lated photons, but, ideally, at only half the rate observed for closely spaced detectors. HBT imaging is attractive for two reasons: First, one does not need to use large telescopes, or technologically challenging amplitude interferometry, and, secondly, atmospheric density fluctuations affect both plane waves in the same way, so they cancel out in the correlation signal.

Two aspects are crucial in this discussion: First, these correlations exist for only brief times, and, the higher the detector time resolution, the more spectral bandwidth can be admitted. The best multilayer interference filters available to date have a bandwidth of about 1/6 to 1/4 nm at a visible wavelength, say, 532 nm. This corresponds to a coherence time of about 5 ps, so a 50-ps-resolving LAPPD will achieve a signal visibility of about 10%, the other 90% being chance correlations. There are many types of detectors with 50 ps resolution, or better, but LAPPD^{TM} also provides the number of pixels that allows to do HBT simultaneously on many stellar objects in the telescope field of view, for example in a stellar cluster. The other aspect is the restriction to just two modes, which enforces amplitude correlations over extended regions and within the coherence time. This restriction to two modes is implicit in the more commonly found explanation of HBT interference as Bosonic bunching, which goes back to Ugo Fano [7], a graphical representation can be found, for example, on the Wikipedia page on HBT (https://en.wikipedia.org/wiki/Hanbury_Brown_and_Twiss_effect).

The reason that the above classical explanation did not invoke quantum statistics is due to the thermal, i.e., classical, statistics of the light sources. Just about any other type of photon statistics will produce intensity interferences that require a full quantum theory, such as that provided by Glauber [8, 9, 10, 11, 12, 13, 14]. For example, the HBT experiment will not work with the Poissonian photon statistics of laser light. LAPPD^{TM} can play a role in experiments using such light, as well, because the fundamental argument does still hold that identifying photons in their modes requires both two-dimensional spatial resolution, as well as a time resolution matched to the reciprocal spectral bandwidth to yield a time-bandwidth product of one. Applications may be found, for example, in optical communication and data processing.

4. Thermal-light Ghost Imaging

Related to the HBT effect is a technique called thermal-light ghost imaging (TGI) [15, 16, 17]. It is based on photon correlations and is capable of producing a clear image even if the optical is disturbed by refractive-index fluctuations (such as air above a hot plate), and conventional images would be severely degraded. Just as in HBT, the time resolution of the imager is important for being able to work with a reasonable spectral bandwidth. For lack of a suitable image sensor, all demonstration experiments of TGI were done either with pseudothermal light [18, 19, 20, 21] or extremely narrow-band light sources, such as hollow-cathode gas-discharge lamps [22], or with a non-imaging sensor that needs to be scanned across the image area [23]. So, TGI to date has been done with either non-natural illumination, or without an imager. Only LAPPD^{TM}, and to a lesser extend certain photodiode arrays, offer the combination of imaging and a time resolution approaching the coherence time of natural thermal light filtered with narrow-band interference filters. Photodiode arrays (SPAD, SiPMT arrays) do offer single-photon sensitivity with some degree of pixellation, and time resolutions of the order of 50 ps. However, to date, none of these approach the number of pixels an LAPPD^{TM} can deliver, and the dark event rates are measured in

tens of thousands per second and mm^2, while those of LAPPD^{TM} are, typically, about a thousand over the entire 40000 mm^2.

A pseudothermal light source consists of a laser and a spinning ground-glass disk. The laser provides the spectrally narrow-band light with coherence times matched (with some technical effort) to the ms resolutions of the CCD or CMOS image sensors being used, and the ground-glass disk provides amplitude fluctuations like those in thermal light, just much slower.

A TGI setup using an LAPPD^{TM} could be modeled on the previously published demonstrations by replacing the pseudothermal light source with light from the sun, a light bulb, etc., restricted with a spatial filter to be a point source (size times divergence of the order of the wavelength). Instead of a CCD chip, an LAPPD^{TM} is used, and the spectral bandwidth of the light is reduced by interference filters placed anywhere in the optical paths to yield a coherence time matched to the detector time resolution. This is shown in Fig. 3, which should be compared to Fig. 1 in reference [21]. It is important to note that thermal light emitted from a source glowing at 5000 K to 10000 K (the visible surface of the sun is at 5777 K), when filtered to a spectral bandwidth matching ms time resolutions, would provide a photon rate per EM mode that would be far too low for correlation experiments. Furthermore, such a narrow-band filtering would require very challenging filters. The time resolution of LAPPD^{TM} is what makes filtered-thermal-light HBT a realistic proposition.
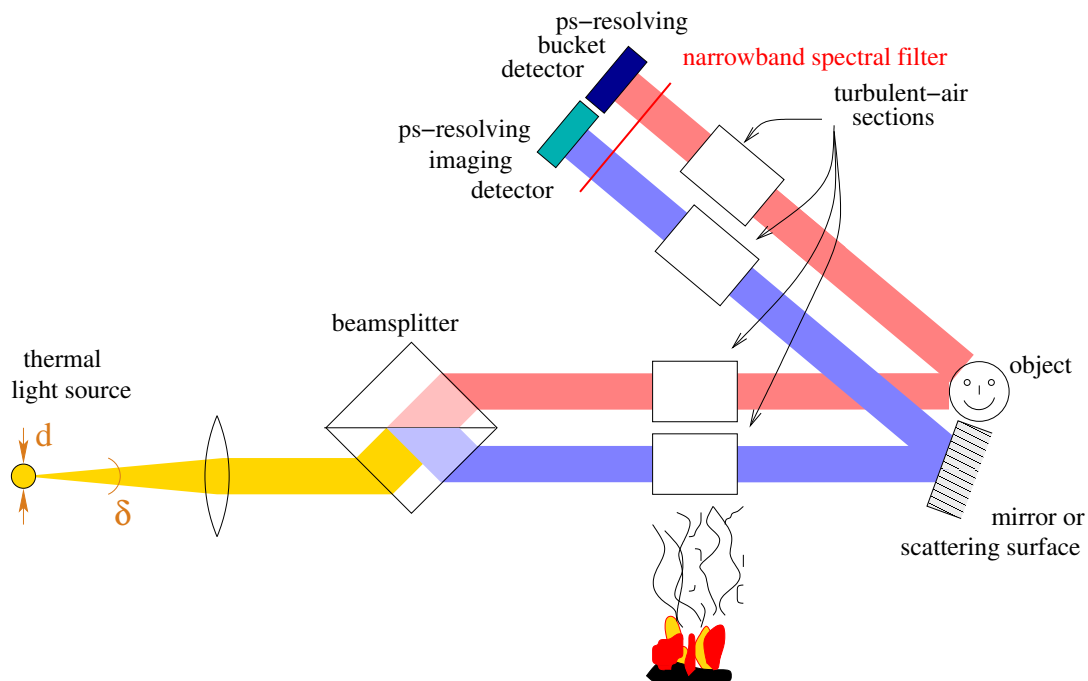

Figure 3: Thermal-light ghost imaging with an LAPPD^{TM} sensor, Compare to Fig. 1 of reference [21]. The main differences are that the CCD sensor is replaced with an LAPPD^{TM}, and a true thermal light source is used, which emits into one transverse mode, i.e., its size d times the emission angle δ is of the order of the wavelength.

5. A Non-Quantum-Optical Application of LAPPD^{TM}

There are other potential applications of LAPPD^{TM} that make full use of its time-resolved imaging capability, and that are classical-optical in nature. An example would be imaging LIDAR, i.e., using a pulsed light source and an LAPPD^{TM} to determine the distance of parts of an object for each pixel to which it is imaged. Imaging LIDAR is an active area of research and development, based mostly on arrays of fast photodiodes (SPDAs or silicon PMTs). LAPPD^{TM} can provide the same time resolution at higher spatial resolution and considerably lower dark-signal rate.

A variation of imaging LIDAR is shown in Fig. where the technique is used to see through fog and smoke by recording, for each pixel, a time series of light intensity after pulsed illumination, and suppressing any low-level signal (fog/smoke), and retaining only stronger ones, which are, presumably, from a solid object.
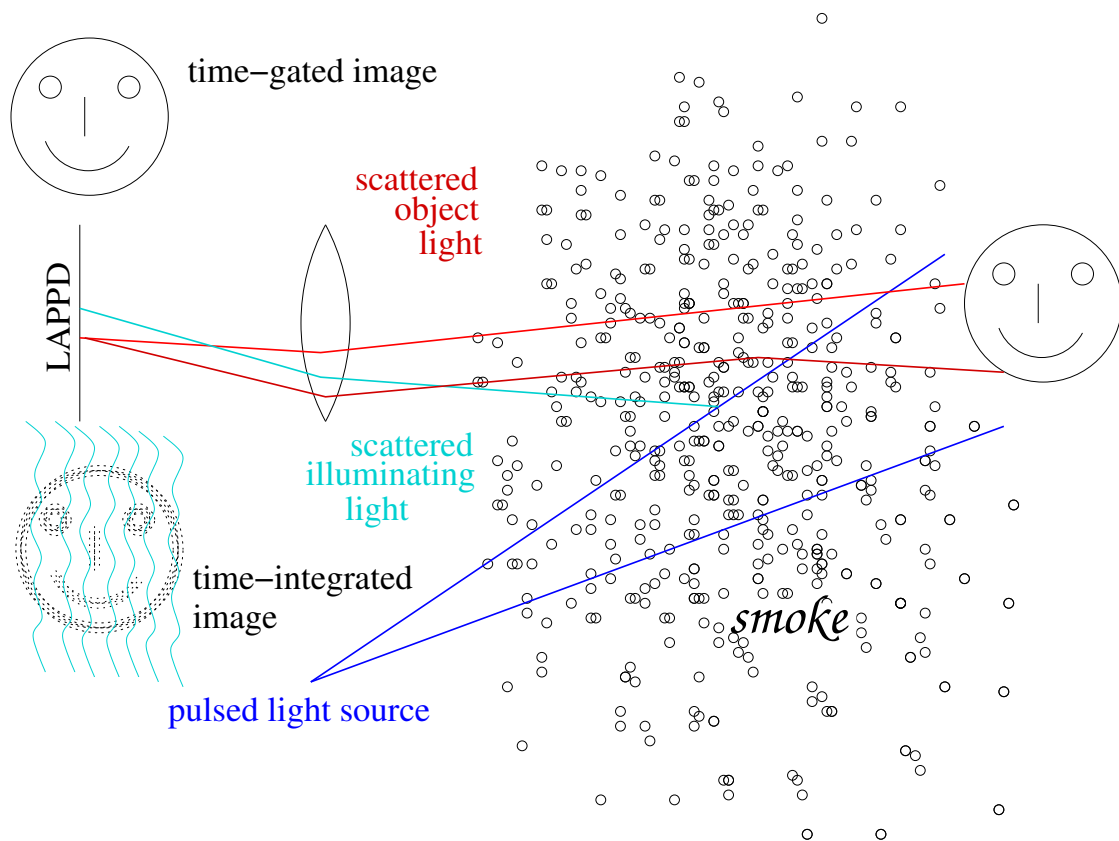

Figure 4: Schematic of the "seeing-through-smoke" application.

Because LAPPD^{TM} can deliver a continuous stream of events on each pixel, one does not have set a time gate around an expected round-trip time of the light (source-object-sensor). Instead, solid objects are identified in the data from their light echo that is stronger than the diffuse scatter from the fog or smoke. By time-correlating strong light echoes between pixels, more certainty about the presence of a solid object can obtained. A possible application of the time-of-flight imaging technique is in firefighting where a common problem is poor visibility in a smoke-filled room.

References

[1] R. Hanbury Brown and R.Q. Twiss. A test of a new type of stellar interferometer on Sirius. *Nature*, 178:1046–1048, 1956.

[2] Bernhard W. Adams, Klaus Attenkofer, Mircea Bogdan, Karen Byrum, Andrey Elagin, and et al. A brief technical history of the large-area picosecond photodetector (LAPPD) collaboration. *arxiv*, 1603:1–46, 2016.

[3] Bernhard Adams, Matthieu Chollet, Andrey Elagin, Eric Oberla, Alexander Vostrikov, Matthew Wetstein, Razib Obaid, and Preston Webster. Invited article: A test-facility for large-area microchannel plate detector assemblies using a pulsed sub-picosecond laser. *Rev. Sci. Instrum.*, 84:061301, 2013.

[4] B.W. Adams, A. Elagin, H.J. Frisch, R. Obaid, E. Oberla, A. Vostrikov, R.G. Wagner, J. Wang, and M. Wetstein. Timing characteristics of large area picosecond photodetectors. *Nucl. Instrum. Methods A*, 795:1–11, 2015.

[5] Glenn R. Jocher, Matthew J. Wetstein, Bernhard Adams, Kurtis Nishimura, and Shawn M. Usman. Multiple-photon disambiguation on stripline-anode micro-channel plates. *Nucl. Instrum. Methods A*, 822:25–33, 2016.

[6] Michael J. Minot, Daniel C. Bennis, Justin L. Bond, Christopher A. Craven, Aileen O'Mahony, and et al. Pilot production & commercialization of LAPPD^{TM}. *Nucl. Instrum. Methods A*, 787:78–84, 2015.

[7] U. Fano. Quantum theory of interference effects in the mixing of light from phase-independent sources. *Am. J. Phys.*, 29:539–545, 1961.

[8] R.J. Glauber. The quantum theory of optical coherence. *Phys. Rev.*, 130:2529–2539, 1963.

[9] R.J. Glauber. Coherent and incoherent states of the radiation field. *Phys. Rev.*, 131:2766–2788, 1963.

[10] U.M. Titulaer and R.J. Glauber. Correlation functions for coherent fields. *Phys. Rev.*, 140:676–682, 1960.

[11] U.M. Titulaer and R.J. Glauber. Density operators for coherent fields. *Phys. Rev.*, 145:1041–1050, 1966.

[12] K.E. Cahill and R.J. Glauber. Density operators and quasiprobability distributions. *Phys. Rev.*, 177:1882–1902, 1969.

[13] Roy J. Glauber. Photon correlations. *Phys. Rev. Lett.*, 10:84–86, 1963.

[14] R.J. Glauber, M. Kleber, A.K. Patnaik, M.O. Scully, and H. Walther. A simple study of photon correlations from Hanbury-Brown and Twiss to Einstein, Podolsky, Rosen and beyond. *J. Phys. B*, 38:S521–S534, 2005.

[15] Yanhua Shih. The physics of ghost imaging. *arxiv_quant-ph*, 0805.1166:1–37, 2008.

[16] A. Gatti, E. Brambilla, M. Bache, and L.A. Lugiato. Correlated imaging, quantum and classical. *Phys. Rev. A*, 70:013802, 2004.

[17] A. Gatti, E. Brambilla, M. Bache, and L.A. Lugiato. Ghost imaging with thermal light: Comparing entanglement and classical correlation. *Phys. Rev. Lett.*, 93:093602, 2004.

[18] W. Martienssen and E. Spiller. Coherence and fluctuations in light beams. *Am. J. Phys.*, 32:919–926, 1964.

[19] Giuliano Scarcelli, Alejandra Valencia, and Yanhua Shih. Experimental study of the momentum correlation of a pseudothermal field in the photon-counting regime. *Phys. Rev. A*, 70:051802, 2004.

[20] Alejandra Valencia, Giuliano Scarcelli, Milena DâĂŹAngelo, and Yanhua Shih. Two-photon imaging with thermal light. *Phys. Rev. Lett.*, 94:063601, 2005.

[21] Ronald E. Meyers, Keith S. Deacon, and Yanhua Shih. Turbulence-free ghost imaging. *Appl. Phys. Lett.*, 98:111115, 2011.

[22] Xi-Hao Chen, Qian Liu, Kai-Hong Luo, and Ling-An Wu. Lensless ghost imaging with true thermal light. *Opt. Lett.*, 34:695–697, 2009.

[23] Sanjit Karmakar, Ronald Meyers, and Yanhua Shih. Ghost imaging experiment with sunlight compared to laboratory experiment with thermal light. *Proc. SPIE*, 8518:1–3, 2012.